*Structural Engineering and Mechanics, Vol. 43, No. 3 (2012) 321-336*
DOI: http://dx.doi.org/10.12989/sem.2012.43.3.321


# A new numerical modelling for evaluating the stress intensity factors in 3-D fracture analysis

Zongjie Cao* and Yongyu Liu[a]

*Department of Aviation Mechanical Engineering, Aviation University of Air Force, Changchun, 130022, China*

*(Received January 13, 2012, Revised May 31, 2012, Accepted June 4, 2012)*

**Abstract.** As an improvement on the isoparametric element method, the derivation presented in this paper is close to that done by Wang (1990) for the 2-D finite element. We extend this idea to solve 3-D crack problems in this paper. A new displacement modelling is constructed with local solutions of three-dimensional cracks and a quasi-compatible isoparametric element for three-dimensional fracture mechanics analysis is presented. The stress intensity factors can be solved directly by means of the present method without any post-processing. A new method for calculating the stress intensity factors of three-dimensional cracks with complex geometries and loads is obtained. Numerical examples are given to demonstrate the validity of the present method. The accuracy of the results obtained by the proposed element is demonstrated by solving several crack problems. The results illustrate that this method not only saves much calculating time but also increases the accuracy of solutions. Because this quasi-compatible finite element of 3-D cracks contains any singularities and easily meets the requirement of compatibility, it can be easily implemented and incorporated into existing finite element codes.

**Keywords:** crack; stress intensity factor; singular element; finite element method

## 1. Introduction

Fracture mechanics has been an important research field in engineering in the last decades. The interest was induced first by the appearance of catastrophic failures caused by crack propagation and more recently by the need for internal damage evaluation in engineering materials in order to guarantee the safety of existing structures and machines for the longest possible period of time. The computation of the stress intensity factors (SIFs) is an elementary and important problem in fracture mechanics analysis of cracked structures. The number of fracture problem with a close form analytic solution is very small because of the complexities in mathematics. Many inves tigators have used numerical methods to obtain their SIFs so that different numerical methods suitable for these kinds of problems have been presented. The body force method (Isida *et al.* 1985) on the basis of the stress field is only used to solve such problem that its geometry is infinite. The weight function method (Wang *et al.* 1998) is useful for the cases with non-uniform stress fields because of its simplicity and economy. This method is not suitable for the cases that have the complicated

*Corresponding author, Professor, E-mail: zjcao96@sina.com
[a]E-mail: liuyongyu@sina.com

geometry and loads. The boundary element method is a mature numerical method in providing solutions to infinite problems (Dong *et al.* 2002, Chai and Zhang 2000). This method is more accurate and effective, but limited if the geometry and the loads are complex, especially for 3-D fracture problems with multi materials and cracks. The finite element alternating technique (Peng *et al.* 2002) is used for the analytical solution for a 3-D elliptical flaw subjected to the arbitrary crack surface loading. This method has a shortcoming that is only suitable for a single isotropic material structure. In this aspect, the finite element method is an effective alternative for solving elastic problems to finite domain problems (Atluri *et al.* 1975). The regular finite element method is not suitable for solving problems with cracks because of the stress singularity at the crack tip. In order to obtain enough accuracy of solutions, this method needs more dense finite element gridding near the crack tip. So various singular elements have been introduced to account for the required crack tip singularity in order to improve the accuracy of the finite element solutions. Compatible singular elements are constructed by means of moving the edge-center-node of isoparametric elements (Barsoum 1976). In this case, the SIF is usually evaluated by Tracey0s formula (Tracey 1976). Incompatible singular elements (Bradford *et al.* 1984) can be obtained from combining the main terms of Williams expansion and the displacement field of regular element. An approximate superposition method for calculating the stress intensity factor of an infinite plate was introduced to solve stress intensity factor problems with 2D multiple hole-edge cracks (Zhao *et al.* 2012). The complex variable function equations were solved numerically using the so-called curve length coordinate method (Nik *et al.* 2009). A general singular integral formulation is suggested to solve SIFs at the crack tips (Chen and Lin 2010). A numerical solution to solve stress intensity factors for a finite internally cracked plate was discussed with hybrid crack element method (Chen 2011). Fan (2004) and Xiao (2003) use the PUE method to discuss 2-D crack problems. The accuracy of the PUE solutions is very high because the PUE method uses a higher order approximation function in solving the stress intensity factors at crack tips. But this method increases additive nodal degrees of freedoms in formulation, which increases computational time and cost. Especially it is very difficult to treat the compatible condition between two kinds of elements. Wang (1990) and Cao (2004) formulate quasi-compatible singular elements by an improvement on the isoparametric element, but the problem about problems with 3-D cracks are not mentioned. Influence coefficients for plates containing an elliptical crack with a wide range of the parameters were presented (Delliou and Barthelet 2007). The effect of clamping force and friction coefficient on SIF of a crack single or double lapped joints using 3D finite element method had been studied (Sallam *et al.* 2011).

Each of the existing methods has its merits and demerits. As an improvement on the isoparametric element method, the derivation presented here is close to that done by Wang (1990) for the 2-D finite element, by Cao (2004) for blunt cracks and by Cao and Kuang (2008) for piezoelectric materials with 2-D cracks. We extend this idea to solve the problems with three dimensional cracks. In this paper, the local solutions of 3-D crack fields are introduced. A new singular element of 3-D crack problems is constructed, and a new method for calculating stress intensity factors of 3-D crack problems is presented. This paper proposes a new and more generally formulated method of 3-D quasi-compatible elements that can contain any singularities and easily meet the requirement of compatibility. This method can be widely used in the numerical analysis of 3-D crack fields in engineering. Numerical examples of the applications illustrate the validity of the present method.

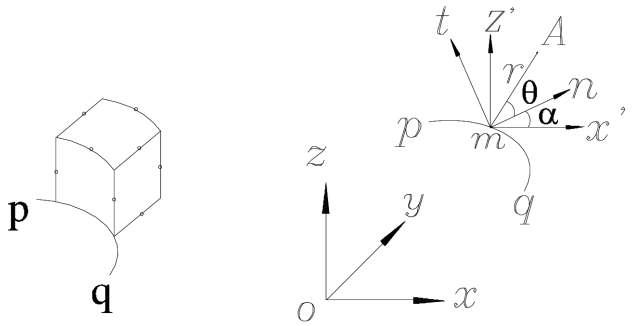


(a) (b)

Fig. 1 A singular element at the crack front

## 2. The displacement model of the 3-D singular element

An arbitrary crack shape in a three-dimensional solid is shown in Fig. 1(a). *pq* is its crack front. Elements located at the crack front are selected as singular elements.

Others are regarded as regular elements. The singular displacement field ($\mathbf{u}_\lambda$) in these singular elements can be expressed as follows

$$\mathbf{u}_\lambda = \mathbf{u}_\lambda^* + \Delta\mathbf{u}_\lambda \tag{1}$$

As shown in Eq. (1), this displacement field is divided into two parts. The first part ($\mathbf{u}_\lambda^*$) can be expressed by the isoparametric interpolation. The second part, $\Delta\mathbf{u}_\lambda$ in Eq. (1), does not include in the displacement field obtained by the isoparametric interpolation.

$$\mathbf{u}_\lambda^* = \mathbf{N}\mathbf{q}_\lambda \tag{2}$$

$$\Delta\mathbf{u}_\lambda = \mathbf{u}_\lambda - \mathbf{N}\mathbf{q}_\lambda \tag{3}$$

where $\mathbf{N}$ is the shape function matrix of the isoparametric element; $\mathbf{q}_\lambda$ is the local nodal displacement array formed by the value of $\mathbf{u}_\lambda$ at the nodes of the singular elements. The general form of the displacement model of singular elements is derived by combining $\Delta\mathbf{u}_\lambda$ of Eq. (3) with the displacement field of the isoparametric element as follows

$$\mathbf{u} = \mathbf{N}\mathbf{q} + (\mathbf{u}_\lambda - \mathbf{N}\mathbf{q}_\lambda) \tag{4}$$

where $\mathbf{q}$ is the nodal displacement array. An arbitrary 3-D crack problem is shown in Fig. 1(b). ($x$, $y$, $z$) is the global coordinate. ($n$, $t$, $z'$) is the local coordinate. $n$ and $t$ are along the normal and tangent directions at the point $m$ on the crack front, $z'$ is orthogonal to the ($n$, $t$) plane. The transposition matrix between the local and global coordinates is

$$\beta = \begin{bmatrix} l_1 & m_1 & n_1 \\ l_2 & m_2 & n_2 \\ l_3 & m_3 & n_3 \end{bmatrix} \tag{5}$$

where $l_i$, $m_i$ and $n_i$ ($i = 1, 2, 3$) are directional cosines between local coordinate axes ($n$, $t$, $z'$) and global coordinate axes ($x$, $y$, $z$), respectively. When $z'$-axis and $z$-axis have the same direction, Eq. (5) can be simplified as

$$\beta = \begin{bmatrix} \cos\alpha & \sin\alpha & 0 \\ -\sin\alpha & \cos\alpha & 0 \\ 0 & 0 & 1 \end{bmatrix} \tag{6}$$

where $\alpha$ is the angle between $n$ and $x$ axes. The local displacement, strain and stress fields ($\sigma_\lambda$, $\varepsilon_\lambda$ and $\mathbf{u}_\lambda$) at the point $A$ near the crack front in the global coordinate can be expressed

$$\mathbf{u}_\lambda = \mathbf{A}_L(r, \theta, \alpha)\lambda_m \tag{7}$$

$$\varepsilon_\lambda = \mathbf{A}_M(r, \theta, \alpha)\lambda_m \tag{8}$$

$$\sigma_\lambda = \mathbf{A}_\lambda(r, \theta, \alpha)\lambda_m \tag{9}$$

$$\lambda_m = [\lambda_{mI}, \lambda_{mII}, \lambda_{mIII}]^T \tag{10}$$

where $\mathbf{A}_L(r, \theta, \alpha)$, $\mathbf{A}_M(r, \theta, \alpha)$ and $\mathbf{A}_\lambda(r, \theta, \alpha)$ are the angle distributed function matrices.

$$\mathbf{A}_L(r, \theta, \alpha) = \frac{6-8\nu}{4\mu}\sqrt{\frac{r}{2}}\times$$

$$\begin{bmatrix} \cos\left(\frac{\theta}{2}+\alpha\right)-\cos\left(\frac{\theta}{2}-\alpha\right)-\cos\left(\frac{3\theta}{2}-\alpha\right) & \sin\left(\frac{\theta}{2}+\alpha\right)+3\sin\left(\frac{\theta}{2}-\alpha\right)+\sin\left(\frac{3\theta}{2}-\alpha\right) & 0 \\ \sin\left(\frac{\theta}{2}+\alpha\right)+\sin\left(\frac{\theta}{2}-\alpha\right)-\sin\left(\frac{3\theta}{2}+\alpha\right) & -\cos\left(\frac{\theta}{2}+\alpha\right)+3\cos\left(\frac{\theta}{2}-\alpha\right)-\cos\left(\frac{3\theta}{2}+\alpha\right) & 0 \\ 0 & 0 & \frac{4\sqrt{4}\sin\frac{\theta}{2}}{6-8\nu} \end{bmatrix}$$

$$\mathbf{A}_M(r, \theta, \alpha) = \frac{1+\nu}{4E\sqrt{2r}}\times$$

$$\begin{bmatrix} \left[(3-8\nu)\cos\frac{\theta}{2}+\cos\frac{5\theta}{2}\right]\cos^2\alpha & \left[(-7+8\nu)\sin\frac{\theta}{2}-\sin\frac{5\theta}{2}\right]\cos^2\alpha & 4\sin\frac{\theta}{2}\sin2\alpha \\ \left[(3+8\nu)\cos\frac{\theta}{2}+\cos\frac{5\theta}{2}\right]\sin^2\alpha & \left[(-7+8\nu)\sin\frac{\theta}{2}-\sin\frac{5\theta}{2}\right]\sin^2\alpha & -4\sin\frac{\theta}{2}\sin2\alpha \\ (5-8\nu)\cos\frac{\theta}{2}-\cos\frac{5\theta}{2} & (-1+8\nu)\sin\frac{\theta}{2}+\sin\frac{5\theta}{2} & 0 \\ \left[(3-8\nu)\cos\frac{\theta}{2}+\cos\frac{5\theta}{2}\right]\sin2\alpha & -\left[(7-8\nu)\sin\frac{\theta}{2}+\sin\frac{5\theta}{2}\right]\sin2\alpha & -8\sin\frac{\theta}{2}\cos2\alpha \\ 2\left(\sin\frac{5\theta}{2}-\sin\frac{\theta}{2}\right)\cos\theta & 2\left(3\cos\frac{\theta}{2}+\cos\frac{5\theta}{2}\right)\cos\theta & -8\cos\frac{\theta}{2}\sin\alpha \\ 2\left(\sin\frac{5\theta}{2}-\sin\frac{\theta}{2}\right)\sin\theta & 2\left(3\cos\frac{\theta}{2}+\cos\frac{5\theta}{2}\right)\sin\theta & 8\cos\frac{\theta}{2}\cos\alpha \end{bmatrix}$$

$$\mathbf{A}_\lambda(r,\theta,\alpha) = \frac{1}{4\sqrt{2r}} \times$$

$$\begin{bmatrix}
\left[3\cos\frac{\theta}{2}+\cos\frac{5\theta}{2}\right]\cos^2\alpha+8\nu\cos\frac{\theta}{2}\sin^2\alpha & -\left(7\sin\frac{\theta}{2}+\sin\frac{5\theta}{2}\right)\cos^2\alpha-8\nu\sin\frac{\theta}{2}\sin^2\alpha & 4\sin\frac{\theta}{2}\sin 2\alpha \\
\left[3\cos\frac{\theta}{2}+\cos\frac{5\theta}{2}\right]\sin^2\alpha+8\nu\cos\frac{\theta}{2}\cos^2\alpha & -\left(7\sin\frac{\theta}{2}+\sin\frac{5\theta}{2}\right)\cos^2\alpha-8\nu\sin\frac{\theta}{2}\cos^2\alpha & -4\sin\frac{\theta}{2}\sin 2\alpha \\
5\cos\frac{\theta}{2}\cos\frac{5\theta}{2} & -\sin\frac{\theta}{2}+\sin\frac{5\theta}{2} & 0 \\
\frac{1}{2}\left[(3-8\nu)\cos\frac{\theta}{2}+\cos\frac{5\theta}{2}\right]\sin\alpha & -\frac{1}{2}\left[(7-8\nu)\sin\frac{\theta}{2}+\sin\frac{5\theta}{2}\right]\sin 2\alpha & -4\sin\frac{\theta}{2}\cos 2\alpha \\
-\left(\sin\frac{\theta}{2}-\sin\frac{5\theta}{2}\right)\cos\alpha & \left(3\cos\frac{\theta}{2}+\sin\frac{5\theta}{2}\right)\cos\alpha & -4\cos\frac{\theta}{2}\sin\alpha \\
-\left(\sin\frac{\theta}{2}-\sin\frac{5\theta}{2}\right)\sin\alpha & \left(3\cos\frac{\theta}{2}+\sin\frac{5\theta}{2}\right)\sin\alpha & -4\cos\frac{\theta}{2}\cos\alpha
\end{bmatrix}$$

$\lambda_m$ is the SIF of the point m which can be determined by the displacement field. The SIFs of the 3-D crack are dependent on the position and continuously vary along the line of the crack front. So the quadric interposition function is used to simulate the variation of SIFs in the element, i.e.

$$\lambda_m = \mathbf{L}\lambda^e \tag{11}$$

where $\mathbf{L}$ is quadric interposition function matrix of SIFs; superscript $e$ expresses the element; $\lambda^e$ is the stress intensity factor arrayin the element.

$$\lambda^e = [\lambda_1, \lambda_2, \ldots, \lambda_p]^T \tag{12}$$

where $p$ is the nodal number at the crack front to a singular element; $\lambda_i$ is the stress intensity factor array of the $i$th node at the crack front in the element.

$$\lambda_i = [\lambda_{iI}, \lambda_{iII}, \lambda_{iIII}]^T \tag{13}$$

Substituting Eq. (11) into Eqs. (7), (8) and (9), local displacement, stress and strain fields of the element can be reduced into the following forms

$$\mathbf{u}_\lambda = \mathbf{A}_L(r,\theta,\alpha)\mathbf{L}\lambda^e \tag{14}$$

$$\varepsilon_\lambda = \mathbf{A}_M(r,\theta,\alpha)\mathbf{L}\lambda^e \tag{15}$$

$$\sigma_\lambda = \mathbf{A}_\lambda(r,\theta,\alpha)\mathbf{L}\lambda^e \tag{16}$$

Substituting Eq. (14) into Eq. (4), the following equation can be obtained

$$\mathbf{u} = \mathbf{N}\mathbf{q} + [\mathbf{A}_L(r,\theta,\alpha)\mathbf{L}\lambda^e - \mathbf{N}\mathbf{q}_\lambda] \tag{17}$$

$$\mathbf{q}_\lambda = \overline{\mathbf{A}}_L(r,\theta,\alpha)\overline{\lambda} = \overline{\mathbf{A}}_L(r,\theta,\alpha)\overline{\mathbf{L}}\lambda^e \tag{18}$$

$$\overline{\mathbf{A}}_L(r,\theta,\alpha) = [\overline{\mathbf{A}}_L(r_1,\theta_1,\alpha_1), \overline{\mathbf{A}}_L(r_2,\theta_2,\alpha_2), \overline{\mathbf{A}}_L(r_p,\theta_p,\alpha_p)]^T \tag{19}$$

where $\bar{A}_L(r_i, \theta_i, \alpha_i)$ is the sub-matrix formed by $\mathbf{A}_L(r, \theta, \alpha)$ at the $i$th node. Substituting Eq. (18) into Eq. (17), the new displacement model of the 3-D singular element can be obtained

$$\mathbf{u} = \mathbf{N}\mathbf{q} + [\mathbf{A}_L(r, \theta, \alpha)\mathbf{L} - \mathbf{N}\bar{\mathbf{A}}_L(r, \theta, \alpha)\bar{\mathbf{L}}]\lambda^e \tag{20}$$

## 3. Finite element formulation

There are NE elements in the entire domain, where there are $R$ singular elements and (NE-R) regular elements. Then global displacement field of the entire domain can be expressed as

$$\mathbf{u} = \begin{cases} \mathbf{N}\mathbf{q} + \mathbf{N}_\lambda \lambda^e, & j \le R \\ \mathbf{N}\mathbf{q}, & j > R \end{cases} \tag{21}$$

where $\mathbf{N}_\lambda = \mathbf{A}_L(r, \theta, \alpha)\mathbf{L} - \mathbf{N}\bar{\mathbf{A}}_L(r, \theta, \alpha)\bar{\mathbf{L}}$. The convergence criterion of the displacement method requires that the displacement model of elements meets the perfect and compatible conditions. The displacement model of element Eq. (20) is perfect. As to the compatible condition Eq. (21), we know that the entire region consists oftwo kinds of elements, namely regular elements and singular elements. There are three types of element boundaries:

(a) the boundary between singular elements;

(b) the boundary between regular elements;

(c) the boundary between the singular and regular elements.

For boundaries (a) and (b), the compatible condition is strictly fulfilled. As for (c), the compatible condition is met only at the nodes. For the boundary between nodes, the compatible condition is fulfilled in the follow two senses: (i) when the element dimension tends to zero, the second term in the displacement model (20) disappears and the compatible condition is guaranteed; (ii) when the boundary nodes of singular elements increase, the second term of Eq. (20) tends to zero. So the compatible condition is approximately fulfilled and the boundary between the two kinds of elements is quasi-compatible. The convergence of present elements is guaranteed.

With the relation between the strain and stress, we have

$$\varepsilon = \mathbf{E}^T(\nabla)\mathbf{u} \tag{22}$$

where $\mathbf{E}^T(\nabla)$ is the differential operator.

$$\mathbf{E}^T(\nabla) = \begin{bmatrix} \frac{\partial}{\partial x} & 0 & 0 \\ 0 & \frac{\partial}{\partial y} & 0 \\ 0 & 0 & \frac{\partial}{\partial z} \\ \frac{\partial}{\partial y} & \frac{\partial}{\partial x} & 0 \\ & \frac{\partial}{\partial z} & \frac{\partial}{\partial y} \\ \frac{\partial}{\partial z} & 0 & \frac{\partial}{\partial x} \end{bmatrix} \tag{23}$$

Substituting Eq. (21) into Eq. (22), the following equation can be obtained

$$\varepsilon = \begin{cases} \mathbf{Bq} + \mathbf{B}_\lambda \lambda^e, & j \le R \\ \mathbf{Bq}, & j > R \end{cases} \tag{24}$$

where $\mathbf{B}_\lambda$ is the singular strain matrix corresponding to the singular strain field near the crack front. $\mathbf{B} = \mathbf{E}^T(\nabla)\mathbf{N}$, $\mathbf{B}_\lambda = \mathbf{E}^T(\nabla)\mathbf{N}_\lambda$. According to the relation between stress and strain, the following equation can be obtained

$$\sigma = \begin{cases} \mathbf{DBq} + \mathbf{DB}_\lambda \lambda^e, & j \le R \\ \mathbf{DBq}, & j > R \end{cases} \tag{25}$$

where $\mathbf{D}$ is the elastic matrix. According to the minimum potential energy principle, we have

$$\pi = \sum_{j=1}^{NE} \left( \int_{\Omega e} \frac{1}{2} \varepsilon^T \sigma d\Omega - \int_{\Omega e} \mathbf{u}^T \mathbf{f} d\Omega - \int_{\Gamma 2e} \mathbf{u}^T \overline{T} d\Gamma \right) \tag{26}$$

Substituting Eqs. (21), (24) and (25) into Eq. (26), we have

$$\pi = \sum_{j=1}^{R} \left\{ \mathbf{q}^T \left( \int_{\Omega e} \mathbf{B}^T \mathbf{D} \mathbf{B}_\lambda d\Omega \right) \lambda + \frac{1}{2} \lambda^T \left( \int_{\Omega e} \mathbf{B}_\lambda^T \mathbf{D} \mathbf{B}_\lambda d\Omega \right) \lambda - \lambda^T \left( \int_{\Omega e} \mathbf{N}_\lambda^T \mathbf{f} d\Omega + \int_{\Gamma 2e} \mathbf{N}_\lambda^T \overline{T} d\Gamma \right) \right\}$$

$$+ \sum_{j=1}^{NE} \times \left\{ \frac{1}{2} \left( \mathbf{q}^T \left( \int_{\Omega e} \mathbf{B}^T \mathbf{D} \mathbf{B} d\mathbf{q} \right) - \mathbf{q}^T \left( \int_{\Omega e} \mathbf{N}^T \mathbf{f} d\Omega + \int_{\Gamma 2e} \mathbf{N}^T \overline{T} d\Gamma \right) \right\} \tag{27}$$

With global matrix symbols, Eq. (27) can be expressed as follows

$$\pi = \frac{1}{2} \mathbf{Q}^T \mathbf{K} \mathbf{Q} + \mathbf{Q}_\lambda^T \mathbf{K}_{NS} \lambda + \frac{1}{2} \lambda^T \mathbf{K}_\lambda \lambda - \mathbf{Q}^T \mathbf{F} - \lambda^T \mathbf{F}_\lambda \tag{28}$$

where

$$\mathbf{K} = \sum_{j=1}^{NE} \left( \frac{1}{2} \int_{\Omega e} \mathbf{B}^T \mathbf{D} \mathbf{B} d\mathbf{q} \right)$$

$$\mathbf{K}_{Ns} = \sum_{j=1}^{R} \int_{\Omega e} \mathbf{B}^T \mathbf{D} \mathbf{B}_\lambda d\Omega$$

$$\mathbf{K}_\lambda = \sum_{j=1}^{R} \left( \frac{1}{2} \int_{\Omega e} \mathbf{B}_\lambda^T \mathbf{D} \mathbf{B}_\lambda d\Omega \right)$$

$$\mathbf{F} = \sum_{j=1}^{NE} \left( \int_{\Omega e} \mathbf{N}^T \mathbf{f} d\Omega + \int_{\Gamma 2e} \mathbf{N}^T \overline{\mathbf{T}} d\Gamma \right)$$

$$\mathbf{F}_\lambda = \sum_{j=1}^{R} \left( \int_{\Omega e} \mathbf{N}_\lambda^T \mathbf{f} d\Omega + \int_{\Gamma 2e} \mathbf{N}_\lambda^T \overline{\mathbf{T}} d\Gamma \right)$$

where $\mathbf{Q}$ is the global displacement array; $\mathbf{Q}_\lambda$ is the global displacement array of singular elements, $\mathbf{Q}_\lambda \in \mathbf{Q}$; $\lambda$ is the stress intensity factor array. To group-crack problems, the general form of Eq. (28) is

$$\pi = \frac{1}{2}\mathbf{Q}^T\mathbf{K}\mathbf{Q} + \sum_{i=1}^{G}\mathbf{Q}_{\lambda i}^T\mathbf{K}_{NSi}\lambda^i + \sum_{i=1}^{G}\frac{1}{2}\lambda^{iT}\mathbf{K}_{\lambda i}\lambda^i - \mathbf{Q}^T\mathbf{F} - \sum_{i=1}^{G}\lambda^{iT}\mathbf{F}_{\lambda i} \tag{29}$$

where $\mathbf{F}_{\lambda i}$ is the external force applied on the surface of the $i$th crack, $\lambda^i$ is the column matrix of stress intensity factors at the $i$th crack front and $G$ is the total crack number in the studied region. Because $\mathbf{Q}$ and $\lambda$ are independentv ariables, the following equations can be obtained by the variational principle

$$\mathbf{K}\mathbf{Q} + \sum_{i=1}^{G}\mathbf{K}_{NSi}\lambda^i = \mathbf{F} \tag{30}$$

$$\mathbf{K}_{NSi}^T\mathbf{Q}_{\lambda i} + \mathbf{N}_{\lambda i}\lambda^i = \mathbf{F}_{\lambda i} \tag{31}$$

Eq. (31) can be rewritten as

$$\lambda^i = -\mathbf{K}_{\lambda i}^{-1}(\mathbf{K}_{NSi}^T\mathbf{Q}_{\lambda i} - \mathbf{F}_{\lambda i}) \tag{32}$$

Substituting Eq. (32) into Eq. (30), we have

$$\mathbf{K}'\mathbf{Q} = \mathbf{F}' \tag{33}$$

where $\mathbf{K}' = \mathbf{K} - \sum_{i=1}^{G}\mathbf{K}_{NSi}\mathbf{K}_{\lambda i}^{-1}\mathbf{K}_{NSi}^T$, $\mathbf{F}' = \mathbf{F} - \sum_{i=1}^{G}\mathbf{K}_{NSi}\mathbf{K}_{\lambda i}^{-1}\mathbf{F}_{\lambda i}$. After solving Eq. (33), the SIFs can be directly obtained from Eq. (32) without any post-processing procedure.

## 4. Numerical examples

### 4.1 Comparison with theoretical solutions

The geometry of the specimen containing an embedded elliptical crack is shown in Fig. 2. 2a and 2b are the lengths of the major and minor axes of an elliptical crack, respectively. The Poisson's ratio ($\nu$) is equal to 0.3 and the load is uniform traction applied on the two opposite sides perpendicular to the plane of the crack. $W$, $t$ and $2H$ are the width, thickness and height of the specimen in the $x$, $y$ and $z$ directions, respectively. The theoretical solution of the normal stress intensity factor of an infinite body is defined as follows (Kassir 1966)

$$\lambda_I = \frac{\sigma\sqrt{\pi b}}{\psi(p)}\left[1 - \frac{a^2 - b^2}{a^2}\cos^2\varphi\right]^{1/4} \tag{34}$$

where $\sigma$ is the uniform applied tensile stress at infinite beyond. $\psi(p)$ is an elliptical integral of the second kind. The above expression indicates that $\lambda_I$ varies along the line of the crack front and has

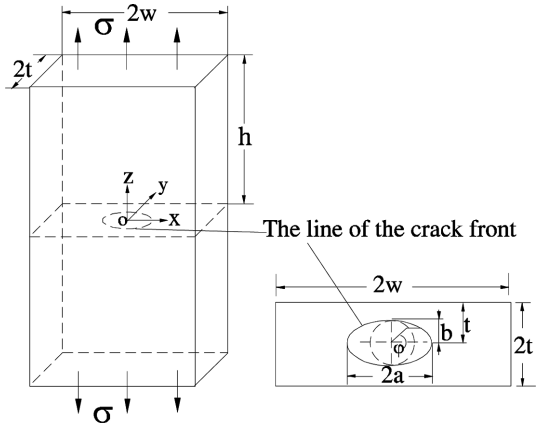


Fig. 2 The plate with an embedded elliptical crack

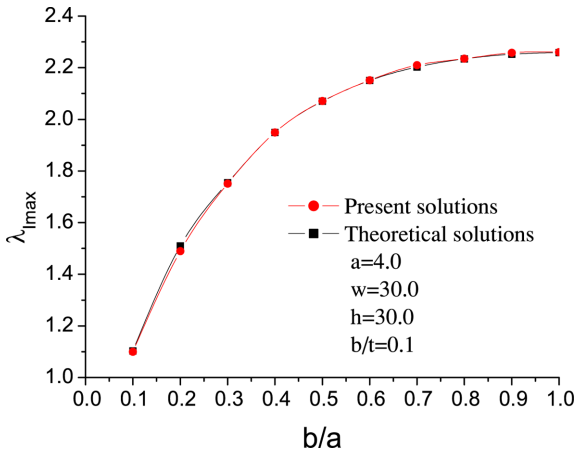


Fig. 3 Mode-I SIFs at the minor axis of the elliptical crack

a maximum value at the end of the minor axis. When $\varphi = \pi/2$, there is the following equation

$$\lambda_{I\max} = \frac{\sigma\sqrt{\pi b}}{\psi(p)} \tag{35}$$

It can be seen from Eq. (35) that $\lambda_{I\max}$ varies with the length of the minor axis of the elliptical crack when the length of the major axis of the elliptical crack is given. The parameters of the crack and structure are chosen to be $a = 4.0$; $a/W = a/h = 0.143$; $b/t = 0.1$; $b/a = 0.1$, 0.2, 0.3, 0.4, 0.5, 0.6, 0.7, 0.8, 0.9 and 1.0, respectively. $\sigma = 1$. Due to the symmetry of the problem, only one eighth of the specimen is discretized. The SIFs at the minor axis of the elliptical crack are calculated as shown in Fig. 3. Fig. 3 shows that the comparison of the stress intensity factors between the present results and the theoretical solutions (Kassir 1966). The results calculated by the present method agree well with those obtained by the theoretical method.

### 4.2 Analysis of element characteristics

The geometry of the specimen containing an embedded elliptical crack is shown in Fig. 2. The stress intensity factor of an arbitrary point in an embedded elliptical crack (Kuang 2002) is

$$\lambda_I = MI\sigma\sqrt{\pi b/Q_0}, \quad Q_0 = \begin{cases} 1.0 + 1.464\left(\frac{b}{a}\right)^{1.65} & \frac{b}{a} \le 1 \\ 1.0 + 1.464\left(\frac{a}{b}\right)^{1.65} & \frac{b}{a} \ge 1 \end{cases} \tag{36}$$

where $MI$ is the normalized stress intensity factor of an arbitrary point in an embedded elliptical crack; $Q_0$ is the crack shape factor. Due to the symmetry of the problem, only one eighth of the specimen is studied. Some main computation results with various Gauss' point numbers can be seen

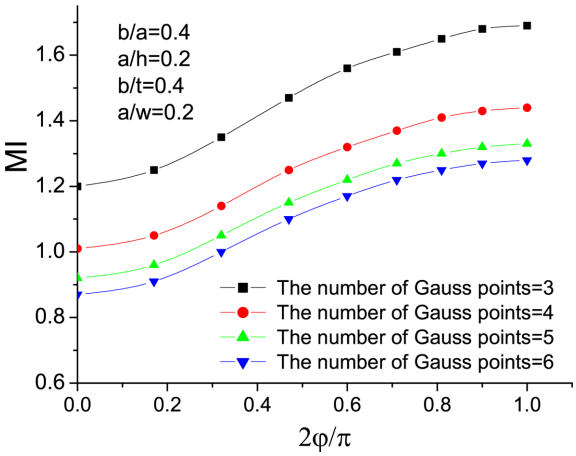


Fig. 4 Computation results vs Gauss' numbers

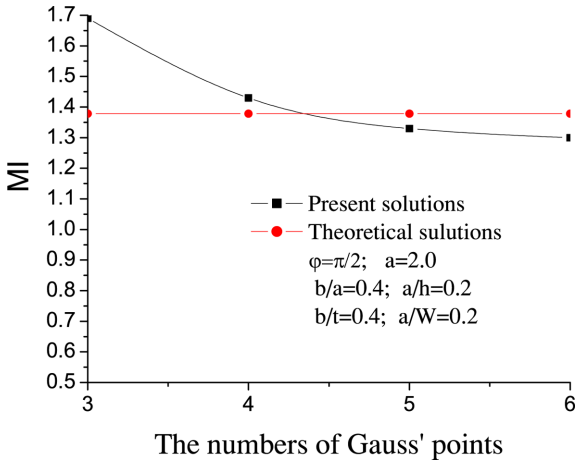


Fig. 5 Computation results vs Gauss' numbers

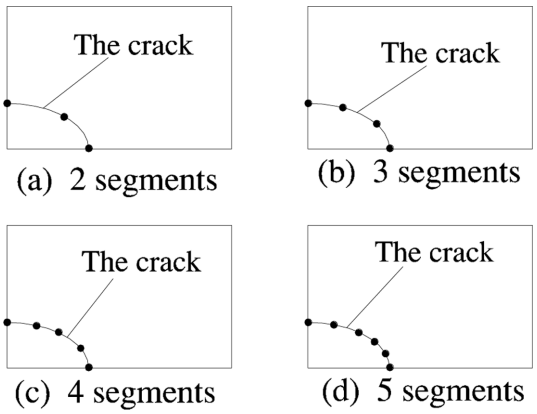


Fig. 6 The numbers of segments at the crack front

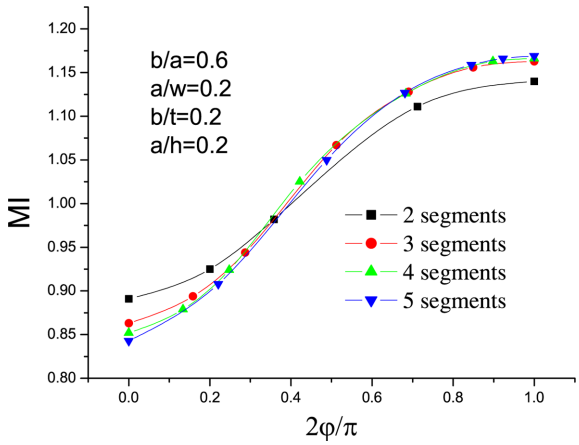


Fig. 7 Computation results vs the numbers of segments on the line of the crack front

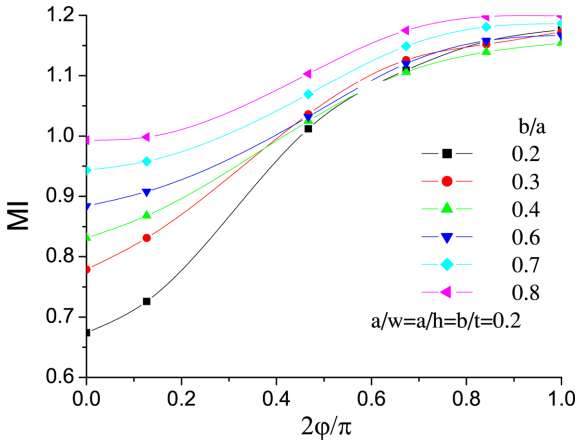


Fig. 8 The inuence of various ratio of *b/a* on the results

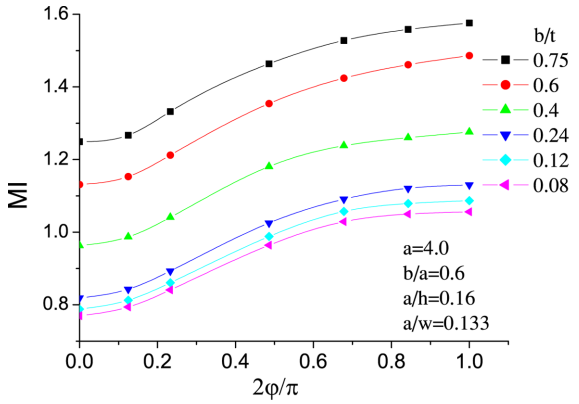


Fig. 9 The influence of structural sizes on the results

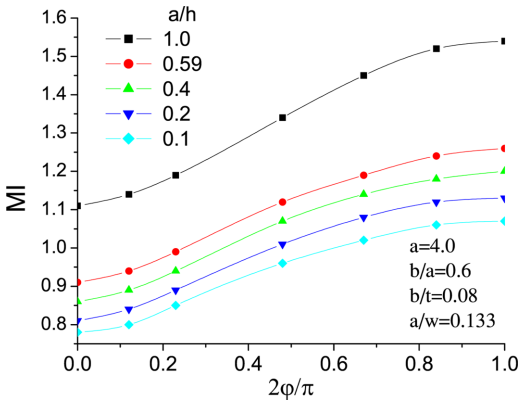


Fig. 10 The influence of structural sizes on the results

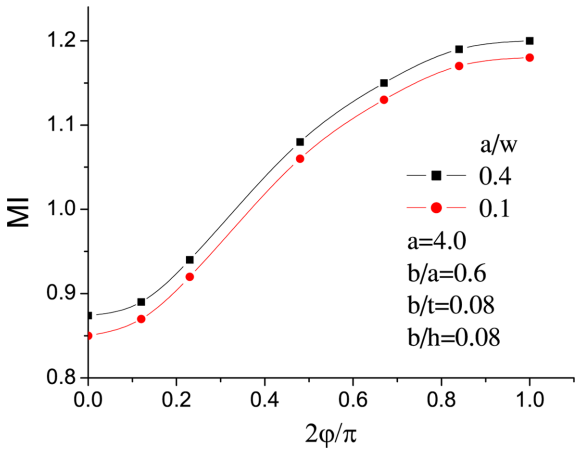


Fig. 11 The influence of structural sizes on the results

in Figs. 4 and 5. At the internal part of singular elements, Gauss' points should be properly increased because the gradient of stress and strain is great. It can be known from Fig. 5 that the computation results can be more ideal when taking the mean value of $4 \times 4 \times 4$, $5 \times 5 \times 5$ points. The different segments of the cross section in the crack plane are shown in Fig. 6. The computation results with various numbers of segments at the crack front can be seen in Fig. 7. The computation results with various radio of $b/a$ for different positions along the crack front can be seen in Fig. 8. The computation results with different structural sizes for different positions along the crack front can be seen in Figs. 9-11.

### 4.3 Through crack

An elastic specimen with a through crack (Parsons and Hall 1989) is shown in Fig. 12(a). The cross section of the crack plane is shown in Fig. 12(b). Its thickness ($t$), height ($h$) and length ($W$) are equal to 250 mm, 2000 mm and 2000 mm, respectively. Along the height direction, the specimen is subjected to uniform tension, $\sigma = 1$ MN/m$^2$. The Poisson's ratio is $\nu = 0.3$ and Young's

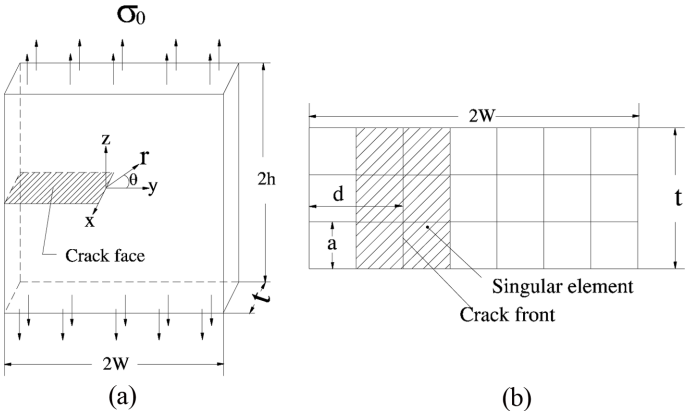


Fig. 12 An elastic specimen with a through crack. (a) specimen (b) singular elements in crack plane

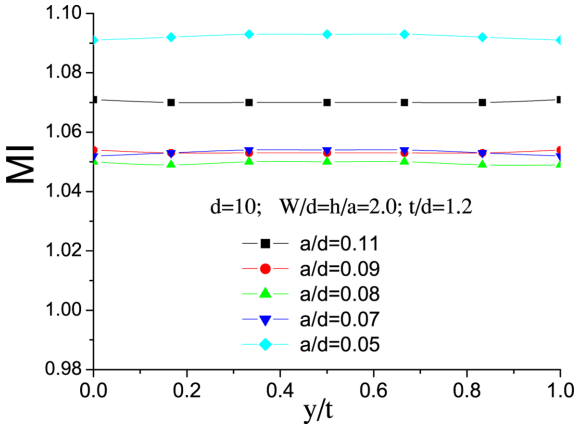


Fig. 13 Computation results vs singular element sizes

Table 1 Comparison ofthe element number, nodal points and degrees of freedoms

| Methods used | Number | | |
|---|---|---|---|
| | Elements | Nodal points | Degrees of freedoms |
| Present method | 20 | 191 | 544 |
| Parsons (1989) | 18432 | | 61659 |
| Tracy (1974) | 522 | 660 | |
| Yamamoto and Sumi (1976) | 480 | 702 | |
| Bloom and Fossen (1976) | 312 | 1655 | |

modulus is equal to 207 $GN/m^2$. Due to the symmetry of the problem, only one quarter of this specimen is discretized. The results of calculation with various singular element sizes for different positions along the crack front can be shown in Fig. 13.

It can be seen from Fig. 7 and Fig. 13 that the influence of element sizes on results is week. This is because the displacement model (Eq. (20)) can entirely include the singularity at crack fronts. Properly to increase the size of singular elements, the accuracy of computation results is still higher. The numbers of elements, nodal points and degrees of freedoms employed by various investigators are listed in Table 1. To compare general efficiency of calculations, the present method seems to have a superiority in engineering applications. This characteristic makes the network dividing of elements only satisfy the requirements for the convergence of the isoparametric element itself and the gradient of normal stress, strain fields in engineering applications.

### *4.4 The surface elliptical crack*

The plate with a semi-elliptical surface crack is loaded by uniform tension as shown in Fig. 14. Fig. 15 shows the comparisons between the present results and Newman-Reju's ones obtained by FEM (Newman 1979) for semi-elliptical surface crack in plates subjected to uniform tension. As can be seen from Fig. 15 that the present results agree closely with Newman-Reju's solutions.

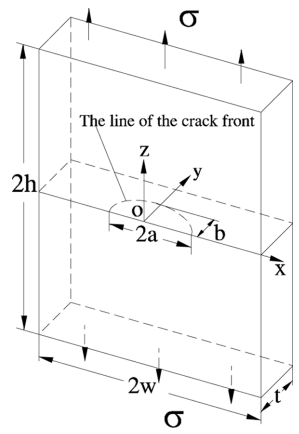


Fig. 14The plate with a semi-elliptical surface crack in a finite thickness plate subjected to uniform tension

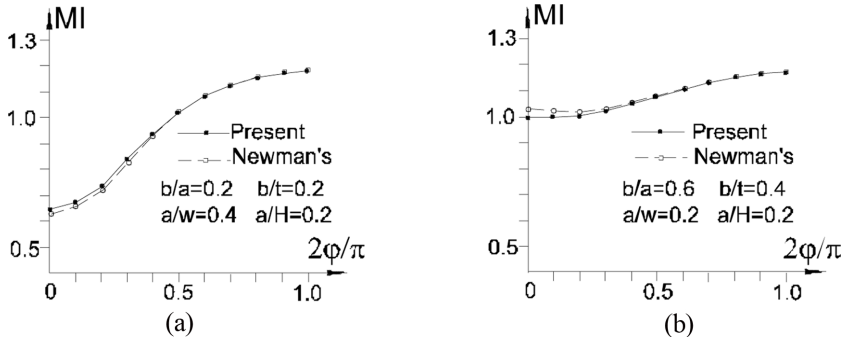


Fig. 15 Comparisons of present computation results with Newman-Reju's solutions

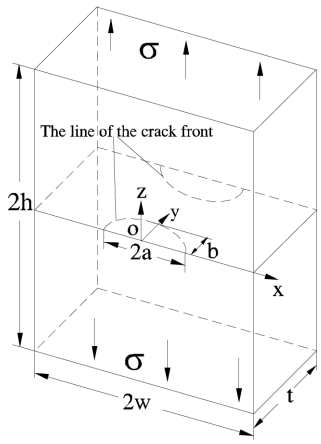


Fig. 16 A finite thickness plate with two semi-elliptical surface cracks

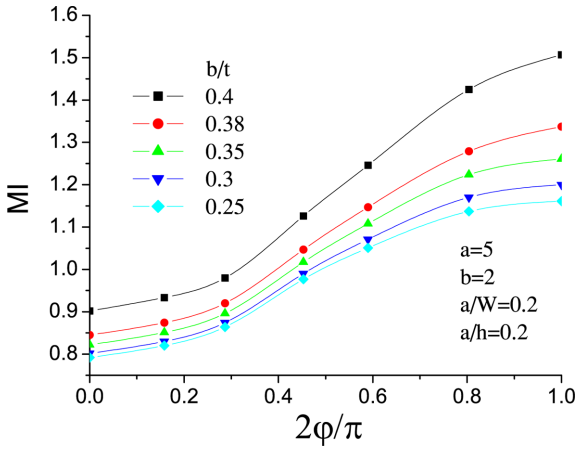


Fig. 17 Mode-I SIFs of a finite thickness plate with two semi-elliptical surface cracks subjected to uniform tension

### 4.5 Multi-cracks

As shown in Fig. 16, a finite thickness plate with two semi-elliptical surface cracks is subjected to uniform tension. The geometry sizes are $a = 5$; $b/a = 0.4$; $a/W = a/h = 0.2$; $b/t = 0.4$, 0.38, 0.35, 0.3 and 0.25, respectively. Fig. 17 shows the stress intensity factors of a finite thickness plate with two semi-elliptical surface cracks subjected to uniform tension.

## 5. Conclusions

A finite element method for three-dimensional linear elastic fracture analysis is established by combining the local solutions of 3-D cracks and the isoparametric elements. From the establishment of the displacement model, theoretical derivation, analysis on the element characteristic and computation results, this method presented in this paper has the following features:

(1) It can solve any 3D brittle linear fracture problems and directly output stress intensity factors without any post-processing procedure.

(2) With the different selection of singular element sizes, Gauss' point numbers, structural sizes etc., results obtained by present method are stable, reliable and highly accurate.

(3) Because this quasi-compatible element of 3-D cracks contains any singularities and easily meets the requirement of compatibility, the size of singular elements along the front of cracks can be larger. In an other word, finite element gridding is not dense, this element not only economize more memory space of computers but also saves calculational time of computers.

(4) Data input and management are almost the same as that for the isoparametric element. It can be easily implemented and incorporated into existing finite element codes in engineering applications.

(5) By combining with any other isoparametric elements, it is very easy to be extended to other fields, such as piezoelectric and ferroelctric intelligent materials.

## References

Atluri, S.N., Kobayashi, A.S. and Nakagaki, M. (1975), "An assumed displacement hybrid finite element method for fracture mechanics", *Int. J. Fract.*, **11**, 257-271.

Barsoum, R.S. (1976), "On the use of isoparametric finite elements in linear fracture mechanics", *Int. J. Numer. Meth. Eng.*, **10**, 25-37.

Bloom, J.M. and Fossen, D.B. (1976), "An evaluation of the 20-node quadratic isoparametric singularity brick element", *Int. J. Fract*., **12**, 161-163.

Bradford, L.G., Dong, S.B., Nicol, D.A.C. and Westmann, R.A. (1984), "A central crack element in fracture mechanics", *Int. J. Fract. Mech*., **24**, 197-207.

Cao, Z.J. and Kuang, Z.B. (2004), "A singular finite element modelling of blunt crack problems and numerical analysis", *ACTA Aeronautica et Astronautica Sinica*, **25**(5), 470-472.

Cao, Z.J. and Kuang, Z.B. (2008), "A finite element modelling for directly determining intensity factors of piezoelectric materials with cracks", *Int. J. Fract.*, **149**, 67-85.

Chai, G.Z. and Zhang, K.D. (2000), "A hybrid boundary element method for three dimensional fracture analysis", *Int. J. Fract.*, **104**, 241-258.

Chen, Y.Z. (2011), "A numerical solution for a finite internally cracked plate using hybrid crack element method", *Struct. Eng. Mech.*, **40**(6), 813-827.

Chen, Y.Z. and Lin, X.Y. (2010), "Numerical solution of singular integral equation for multiple curved branch-cracks", *Struct. Eng. Mech.*, **34**(1), 85-95.
Delliou, P.L. and Barthelet, B. (2007), "New stress intensity factor solutions for an elliptical crack in a plate", *Nucl. Eng. Des.*, **237**, 1395-1405.
Dong, C.Y., Cheung, Y.K. and Lo, S.H. (2002), "A regularized domain integral formulation for inclusion problems of various shapes by equivalent inclusion method", *Comput. Meth. Appl. Mech. Eng.*, **191**, 3411-3421.
Fan, S.C., Liu, X. and Lee, C.K. (2004), "Enriched partition-of-unity finite element method for stress intensity factors at crack Tips", *Comput. Struct.*, **82**, 445-461.
Isida, M., Hirota, K., Noguchi, H. and Yoshida, T. (1985), "Two parallel elliptical cracks in an infinite solid subjected to tension", *Int. J. Fract.*, **17**, 31-48.
Kassir, M.K. and Sih, G.C. (1966), "Three dimensional stress distribution around an elliptical crack under arbitrary loading", *J. Appl. Mech.*, **33**, 601-611.
Kuang, Z.B. and Ma, F.S. (2002), *The Crack Tip Fields*, Xi'an Jiaotong University Publishing House, Xi'an.
Miyazaki, N., Kaneko, H. and Munakata, T. (1989), "Stress intensity analysis of enteracting elliptical cracks using line-spring boundary element method", *Int. J. Ves. Pip.*, **38**, 1-14.
Newman, J.C. and Raju, I.S. (1979), "Stress intensity factors for a wide range of semi-elliptical surface cracks in finite-thickness plates", *Eng. Fract. Mech.*, **11**, 817-829.
Nik Long, N.M.A. and Eshkuvatov, Z.K. (2009), "Hypersingular integral equation for multiple curved cracks problem in plane elasticity", *Int. J. Solids Struct.*, **46**, 2611-2617.
Parsons, I.D. and Hall, J.F. (1989), "A finite element investigation of the elastostatic state near a three dimensional edge crack", *Eng. Fract. Mech.*, **33**(1), 45-63.
Peng, D., Jones, R. and Pitt, S. (2002), "Implementation of a new algorithm for evaluating 3D fracture analysis", *Int. J. Fract.*, **113**, 57-75.
Sallam, H.E.M., El-Sisi, A.E.A., Matar, E.B. and El-Hussieny, O.M. (2011), "Effect of clamping force and friction coefficient on stress intensity factor of cracked lapped joints", *Eng. Fail. Anal.*, **18**, 1550-1558.
Tracey, D.M. (1974), "Finite elements for three-dimensional elastic crack analysis", *Nucl. Eng. Des.*, **26**, 282-290.
Tracey, D.M. (1976), "Discussion of 'on the use of isoparametric finite elements in linear fracture mechanics' by RS Barsoum", *Int. J. Numer. Meth. Eng.*, **10**, 401-403.
Wang, X., Lambert, S.B. and Glink, G. (1998), "Approximate weight functions for embedded elliptical cracks", *Eng. Fract. Mech.*, **59**, 381-392.
Wang, Z.C., Zhang, L.S. and Liu, C.T. (1990), "A new formulated of a quasi-compatible finite element and Its application in fracture mechanics", *Eng. Fract. Mech.*, **37**(6), 1195-1201.
Xiao, Q.Z. and Karihaloo, B.L. (2003), "Direct evaluation of accurate coefficients of the linear elastic crack tip asymptotic field", *Fatigue Fract. Eng. Nater Struct.*, **26**, 719-729.
Yamamoto, Y. and Sumi, Y. (1976), "Stress intensity factors for three-dimensional cracks", *14th Int. Cong. on Theor. and Appl. Mech.,* Delft.
Zhao, J.F., Xie, L.Y., Liu, J.Z and Zhao, Q. (2012), "A method for stress intensity factor calculation of infinite plate containing multiple hole-edge cracks", *Int. J. Fatig.*, **35**, 2-9.